

Supporting information

Molten NaCl-induced MOF-derived Carbon-polyhedron Decorated Carbon-nanosheet with High Defects and High N-doping for Boosting the Removal of Carbamazepine from Water

Dezhi Chen,^{*a} Shoujun Wang,^a Zhiming Zhang,^a Hongying Quan,^{a,b} Yachao Wang,^a Yijie Jiang,^a

Matthew J. Hurlock,^c Qiang Zhang,^{*c}

^a Key Laboratory of Jiangxi Province for Persistent Pollutants Control and Resources Recycle, School of Environmental and Chemical Engineering, Nanchang Hangkong University, Nanchang 330063, China

^b School of Materials Science and Engineering, Nanchang Hangkong University, Nanchang 330063, China

^cDepartment of Chemistry, Washington State University, Pullman, WA 99164-4630

KEYWORDS. Hierarchical structure carbon; adsorption; defect; N doping; interfacial interact.

Section S1

Two kinetic models, including pseudo-first-order kinetic and pseudo-second-order kinetic, were applied to fit the adsorption data of CBZ. The corresponding kinetic models can be expressed as follows Equation S1 and Equation S2, respectively.

$$\ln(q_e - q_t) = \ln q_e - K_1 t \quad (\text{Equation S1})$$

$$\frac{t}{q_t} = \frac{t}{q_e} + \frac{1}{K_2 q_e^2} \quad (\text{Equation S2})$$

where the q_t and q_e (mg g^{-1}) are the amounts of the absorbed CBZ at t time (min) and equilibrium, respectively, and K_1 (min^{-1}) is the pseudo-first-order rate constant of the Equation S1. K_2 ($\text{g mg}^{-1} \text{min}^{-1}$) is the pseudo-second-order rate constant in Equation S2

Section S2

To further evaluate adsorption kinetics of as-prepared sorbents, the adsorption rate (v_a) of sorbents for the removal of CBZ from water was calculated by the Equation S3.

$$v_a = \frac{(C_0 - C_t) V}{m t} \quad (\text{Equation S3})$$

where v_a ($\text{mg g}^{-1} \cdot \text{min}^{-1}$) is the adsorption rate, C_0 (mg L^{-1}) is the initial concentration of CBZ and C_t (mg L^{-1}) is the concentration of CBZ at the time to reach 90% of the maximum adsorption. V (L) is the volume of solution and m (g) is the weight of the adsorbent. t (min) is the time to reach 90% of the maximum adsorption.

Section S3

We use two most common adsorption models to describe the isotherm adsorption behavior of CBZ on HCCs. Langmuir model represents single-layer adsorption, in which the adsorbate is

adsorbed on the adsorbent surface. Freundlich model is an empirical model that represents multi-layer adsorption. The corresponding equations are shown below:

$$\frac{C_e}{q_e} = \frac{C_e}{q_m} + \frac{1}{K_L q_m} \quad (\text{Equation S4})$$

$$\log q_e = \log K_F + \frac{1}{n} \log C_e \quad (\text{Equation S5})$$

where C_e ($\text{mg}\cdot\text{L}^{-1}$) and q_e ($\text{mg}\cdot\text{g}^{-1}$) are the equilibrium concentration and equilibrium amount of adsorbed CBZ, respectively; q_m ($\text{mg}\cdot\text{g}^{-1}$) is the maximum adsorption capacity of adsorbent, and K_L ($\text{L}\cdot\text{mg}^{-1}$) is the Langmuir constant related to the adsorption bond energy. The K_F and n are the Freundlich constants related to the adsorption capacity and intensity of adsorbent.

Section S4

Thermodynamic parameters just like free energy change (ΔG°), enthalpy change (ΔH°) and entropy (ΔS°) were calculated using the following Equation S6 and Equation S7.

$$\Delta G^\circ = -RT \ln K_p \quad (\text{Equation S6})$$

$$\ln K^0 = -\frac{\Delta H^0}{RT} + \frac{\Delta S^0}{R} \quad (\text{Equation S7})$$

Where, the thermodynamic equilibrium constant (K_d) depends on the temperature, Gibb's free energy change (ΔG^0 , kJ mol^{-1}), standard enthalpy change (ΔH^0 , kJ mol^{-1}) and standard entropy change in entropy (ΔS_0 , $\text{J mol}^{-1}\text{K}^{-1}$) to describe the thermodynamic process of adsorption.

When $\Delta G_T < 0$ at temperature T, the reaction is spontaneous, whereas the reaction is not spontaneous at this temperature. Moreover, if ΔH is less than 0 then the reaction is exothermic, otherwise, the adsorption processes is endothermic

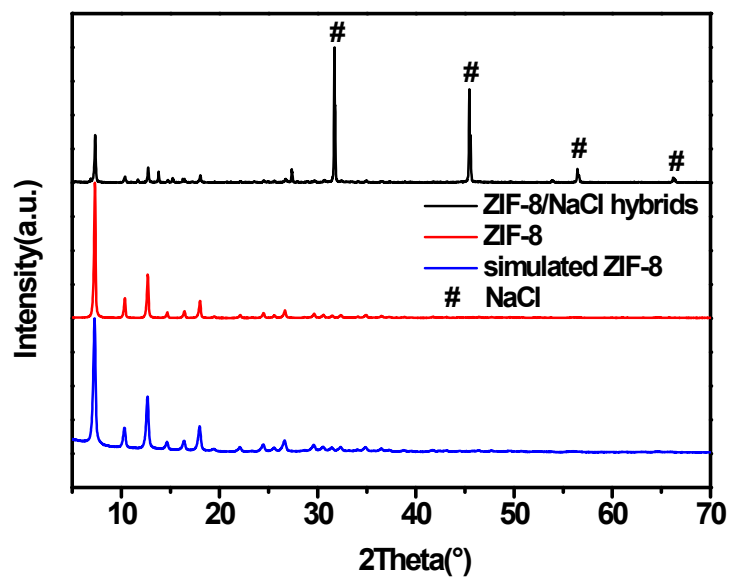


Figure S1. XRD patterns of as-prepared ZIF-8 and ZIF-8/NaCl hybrids

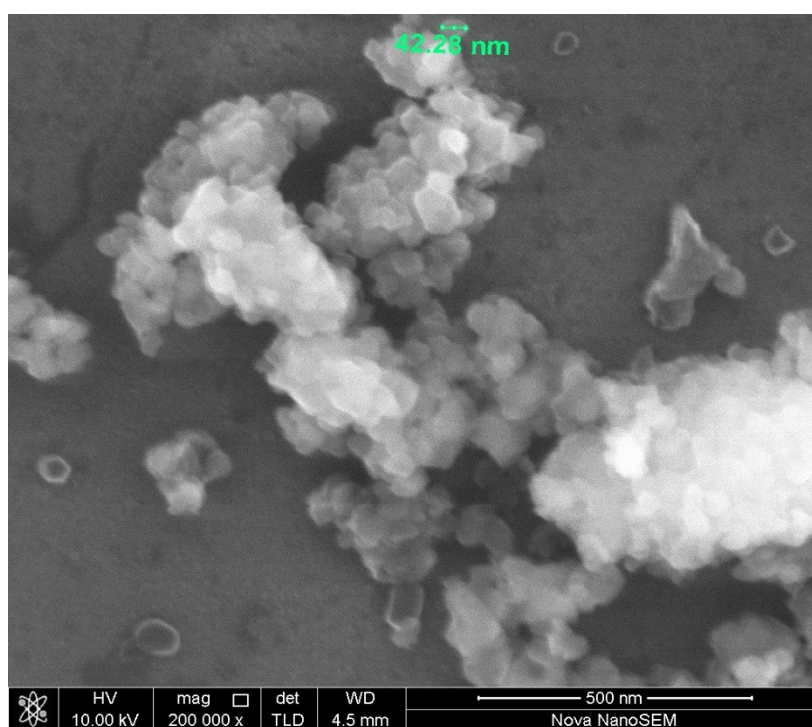


Figure S2. SEM image of as-prepared ZIF-8

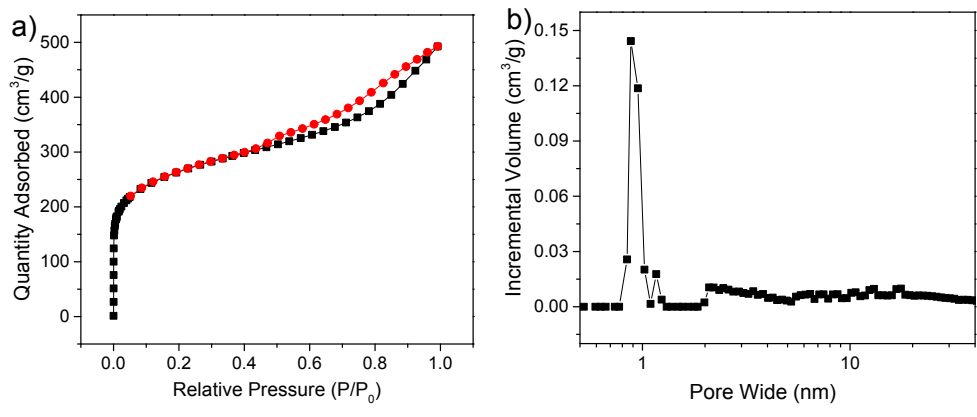


Figure S3. N₂ adsorption-desorption isotherm and pore size distribution of powdered AC.

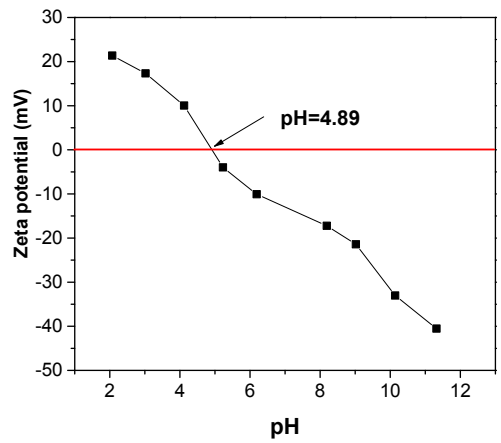


Figure S4. Zeta potential of HCCs.

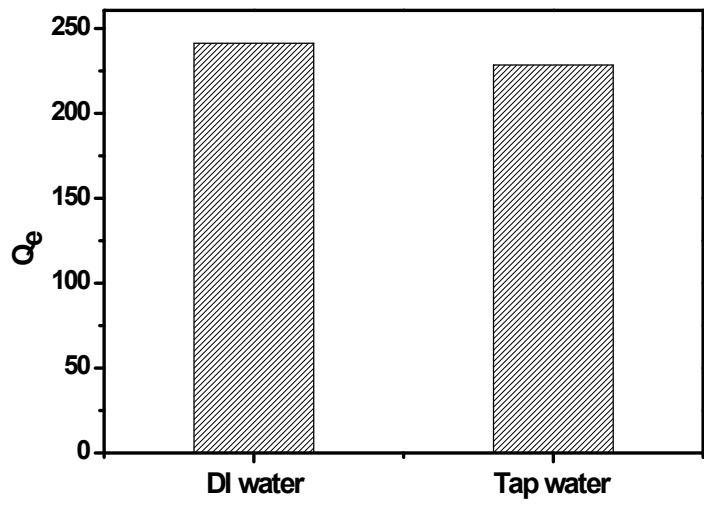


Figure S5. Adsorption amount of CBZ on HCCs from DI water and tap water

Table S1. Pore structure of the as-prepared HCCs, CPs and AC

Sample	S_{BET} (m^2/g)		Pore volume (cm^3/g)	
	Micro	Total	Micro	Total
HCCs	712.2	1026.5	0.482	0.587
CPs	285.1	447.1	0.215	0.283
AC	322.5	866.9	0.334	0.751

Table S2. The atomic conc% of CPs, CBZ, and HCCs before and after adsorption of CBZ from XPS results.

	Atomic conc%		
	C1s (%)	O1s (%)	N1s (%)
CPs	88.31	2.28	9.41
HCCs	85.21	2.33	12.45
HCCs-CBZ	86.55	4.57	8.88
CBZ	84.69	5.44	9.87

Table S3. Kinetic model parameters for the adsorption of CBZ on HCCs, CPs, and AC.

Sorbent	Pseudo-first-order model			Pseudo-second-order model		
	$Q_{\text{e cal}}/$ (mg L^{-1})	$K_1/$ (L mg^{-1})	R^2	$Q_{\text{e cal}}/$ (mg L^{-1})	$K_2/$ (L mg^{-1})	R^2
HCCs	34.53	3.7×10^{-5}	-0.091	216.45	0.00144	0.999
CPs	67.11	0.018	0.967	21.45	0.00638	0.999
AC	6222.00	0.027	0.734	160	0.00110	0.998

Table S4. Adsorption capacity and rate of CBZ on HCCs, CPs, AC and other reported adsorbents.

Adsorbents	CBZ		
	t (min)	Q_t (mg g^{-1})	v_a ($\text{mg g}^{-1} \text{min}^{-1}$)
HCCs	4	202.5	50.63
CPs	30	17.5	0.583
AC	30	142.2	4.74
UiO-66[1]	240	27.8	0.116
KOH-activated biochar[2]	100	250	2.5
CNT-DFB 1.8[3]	720	275	0.382
AC-PS[4]	180	242	1.344
bleached pulp 800-HCl-H ₃ PO ₄ [5]	50	81	1.62
Mesoporous AC[6]	120	162	1.35
GO/MWCNT-COOH[7]	60	147	2.45
AC/Fe ₃ O ₄ [8]	180	102	0.567

* t is the time to reach 90% of the maximum adsorption

Table S5. Thermodynamic parameters for the adsorption of CBZ on HCCs

	T(°C)	lnK°	ΔG° (J mol ⁻¹)	ΔH° (J mol ⁻¹)	ΔS° (mol·K) ⁻¹)
CBZ	25	3.069	-7608.15	-7954.94	-1.21825
	35	2.945	-7544.41		
	45	2.868	-7586.06		

Table S6. Langmuir and Freundlich models parameters of CBZ on HCCs

	Langmuir			Freundlich		
	Q _{max} /(mg/L)	K _L /(L/mg)	R ²	n	K _F /(mg ^{-1/n} L ^{1/n} g ⁻¹)	R ²
25°C	248.76	2.297	0.996	3.902	2.170	0.969
35°C	242.72	1.761	0.989	4.266	2.144	0.968
45°C	240.38	1.342	0.985	3.896	2.104	0.968

Table S7. Parameters of impurity in tap water

Ammonia nitrogen	<0.5 mg L ⁻¹
COD	<5 mg L ⁻¹
Sodium	<200 mg L ⁻¹
Nitrate	<20 mg L ⁻¹
Sulfate	<300 mg L ⁻¹
Total dissolved solids	<1500 mg L ⁻¹
Total number of colonies	<500 CFU mL ⁻¹
pH	≤9.5, ≥6.5

Reference

- [1] C. Chen, D. Chen, S. Xie, H. Quan, X. Luo, L. Guo, Adsorption Behaviors of Organic Micropollutants on Zirconium Metal-Organic Framework UiO-66: Analysis of Surface Interactions, *ACS applied materials & interfaces*, 9 (2017) 41043-41054.
- [2] D. Chen, S. Xie, C. Chen, H. Quan, L. Hua, X. Luo, L. Guo, Activated biochar derived from pomelo peel as a high-capacity sorbent for removal of carbamazepine from aqueous solution, *RSC Advances*, 7 (2017) 54969-54979.
- [3] D. Shan, S. Deng, C. He, J. Li, H. Wang, C. Jiang, G. Yu, M.R. Wiesner, Intercalation of rigid molecules between carbon nanotubes for adsorption enhancement of typical pharmaceuticals, *Chemical Engineering Journal*, 332 (2018) 102-108.
- [4] S. Álvarez-Torrellas, J.A. Peres, V. Gil-Álvarez, G. Ovejero, J. García, Effective adsorption of non-biodegradable pharmaceuticals from hospital wastewater with different carbon materials, *Chemical Engineering Journal*, 320 (2017) 319-329.
- [5] G. Oliveira, V. Calisto, S.M. Santos, M. Otero, V.I. Esteves, Paper pulp-based adsorbents for the removal of pharmaceuticals from wastewater: A novel approach towards diversification, *Sci Total Environ*, 631-632 (2018)

1018-1028.

[6] M.C. Ncibi, M. Sillanpää, Optimizing the removal of pharmaceutical drugs Carbamazepine and Dorzolamide from aqueous solutions using mesoporous activated carbons and multi-walled carbon nanotubes, *Journal of Molecular Liquids*, 238 (2017) 379-388.

[7] N. Cai, P. Larese-Casanova, Sorption of carbamazepine by commercial graphene oxides: a comparative study with granular activated carbon and multiwalled carbon nanotubes, *Journal of colloid and interface science*, 426 (2014) 152-161.

[8] D. Shan, S. Deng, T. Zhao, B. Wang, Y. Wang, J. Huang, G. Yu, J. Winglee, M.R. Wiesner, Preparation of ultrafine magnetic biochar and activated carbon for pharmaceutical adsorption and subsequent degradation by ball milling, *Journal of hazardous materials*, 305 (2016) 156-163.